Virology 488 (2016) 202–215

Contents lists available at ScienceDirect

Virology

journal homepage: www.elsevier.com/locate/yviro

Cell–cell contact promotes Ebola virus GP-mediated infection

Chunhui Miao [a], Minghua Li [a], Yi-Min Zheng [a], Fredric S. Cohen [b], Shan-Lu Liu [a,*]

[a] Department of Molecular Microbiology and Immunology, Bond Life Sciences Center, University of Missouri, Columbia, MO 65211, USA
[b] Department of Molecular Biophysics and Physiology, Rush University Medical Center, Chicago, IL 60612, USA

ARTICLE INFO

Article history:
Received 27 August 2015
Returned to author for revisions
18 November 2015
Accepted 19 November 2015
Available online 3 December 2015

Keywords:
Ebola virus
GP
Cell-to-cell infection

ABSTRACT

Ebola virus (EBOV) is a highly pathogenic filovirus that causes hemorrhagic fever in humans and animals. Here we provide evidence that cell–cell contact promotes infection mediated by the glycoprotein (GP) of EBOV. Interestingly, expression of EBOV GP alone, even in the absence of retroviral Gag-Pol, is sufficient to transfer a retroviral vector encoding Tet-off from cell to cell. Cell-to-cell infection mediated by EBOV GP is blocked by inhibitors of actin polymerization, but appears to be less sensitive to KZ52 neutralization. Treatment of co-cultured cells with cathepsin B/L inhibitors, or an entry inhibitor 3.47 that targets the receptor NPC1 for virus binding, also blocks cell-to-cell infection. Cell–cell contact also enhances spread of rVSV bearing GP in monocytes and macrophages, the primary targets of natural EBOV infection. Altogether, our study reveals that cell–cell contact promotes EBOV GP-mediated infection, and provides new insight into understanding EBOV spread and viral pathogenesis.

Introduction

Ebola virus (EBOV) belongs to the filovirus family and causes severe hemorrhagic fever in humans and animals. The fatality rates of the disease induced by EBOV can reach up to 90%, with currently no effective antiviral drug or FDA-licensed vaccine available (Feldmann and Geisbert, 2011; Hoenen and Feldmann, 2014a). A better understanding of EBOV infection, especially the early stage of viral transmission, would facilitate the development of novel therapeutic approaches to combat this deadly disease.

EBOV infection of a host cell is mediated by its sole glycoprotein, known as GP. GP is synthesized as a precursor (GP0) in the endoplasmic reticulum, cleaved into GP1 and GP2 in the Golgi apparatus, and eventually targeted to the plasma membrane for viral incorporation (Takada et al., 1997; White et al., 2008; Wool-Lewis and Bates, 1999). During this process, EBOV GP is modified by N- and O-linked glycosylation; the exact functions are still not well understood (Dowling et al., 2007; Simmons et al., 2002). In mature virions, EBOV GP exists as a homotrimer, with each monomer composed of GP1 and GP2 subunits that are linked by a disulfide bond and non-covalent interactions (Jeffers et al., 2002; Lee et al., 2008). As is the case for many class I viral fusion proteins, GP1 is responsible for interacting with cellular receptors or cofactors, whereas GP2 is directly involved in fusion of EBOV with target cell membranes (Brindley et al., 2007; Gregory et al., 2011; Hood et al., 2010; Lee et al., 2008; Manicassamy et al., 2005; Wang et al., 2011; Watanabe et al., 2000; Wool-Lewis and Bates, 1999).

The detailed molecular mechanism underlying EBOV GP-mediated infection is currently unknown (White and Schornberg, 2012). However, much evidence has indicated that EBOV enters host cells through macropinocytosis (Hunt et al., 2011; Nanbo et al., 2010; Saeed et al., 2010), a process that is initiated by binding of EBOV GP to attachment factors, such as DC-SIGN and TIM-1 (Alvarez et al., 2002; Kondratowicz et al., 2011; Lin et al., 2003; Marzi et al., 2006; Nanbo et al., 2010). Following the uptake of viral particles into late endosomes and lysosomes, GP1 is cleaved by cellular cysteine proteases, especially cathepsins B (CatB) and L (CatL), resulting in the production of a fusion-competent intermediate (Chandran et al., 2005; Dube et al., 2009; Schornberg et al., 2006) that binds to the recently identified intracellular receptor, Niemann-Pick type C1 (NPC1) (Côté et al., 2011; Kaletsky et al., 2007; Miller et al., 2012). Studies from several groups have shown or suggested that NPC1, low pH, and possibly mild reduction of GP are important for EBOV GP-mediated infection (Bale et al., 2011; Brecher et al., 2012; Gregory et al., 2011; Miller et al., 2012; Schornberg et al., 2006).

Cell-to-cell transmission has been shown to play important roles in the dissemination and pathogenesis of many pathogenic viruses, including HIV and HCV (Brimacombe et al., 2011; Dale et al., 2013; Roberts et al., 2015; Zhong et al., 2013). In this work, we provide evidence that cell–cell contact facilitates infection mediated by EBOV GP and this process requires cellular cathepsins and NPC1. Our work supports the idea that cell-to-cell infection

* Corresponding author.
E-mail address: liushan@missouri.edu (S.-L. Liu).

http://dx.doi.org/10.1016/j.virol.2015.11.019
0042-6822/

may be another means of EBOV spread and could serve as a potential target of viral therapeutics.

Results

Cell–cell contact promotes EBOV GP-mediated retroviral infection

EBOV is a BSL-4 agent; thus, in this study we employed several systems, including retroviral pseudotypes, virus-like particles (VLPs), as well as rVSV that bear GP to determine cell-to-cell infection. For the retroviral system, we co-transfected 293T cells with the pQCXIP retroviral vector encoding a tetracycline-controlled transcription factor (tTA, referred to as Tet-off hereafter), along with plasmids that encode EBOV GP and murine leukemia virus (MLV) Gag-Pol. Following 24 h transfection, donor 293T cells producing pseudovirions were co-cultured with target 293FT cells stably expressing tetracycline-responsive element (TRE)-driven *Gaussia* luciferase (293FT/TRE-GLuc); cell-to-cell infection efficiency was assayed by measuring the GLuc activity

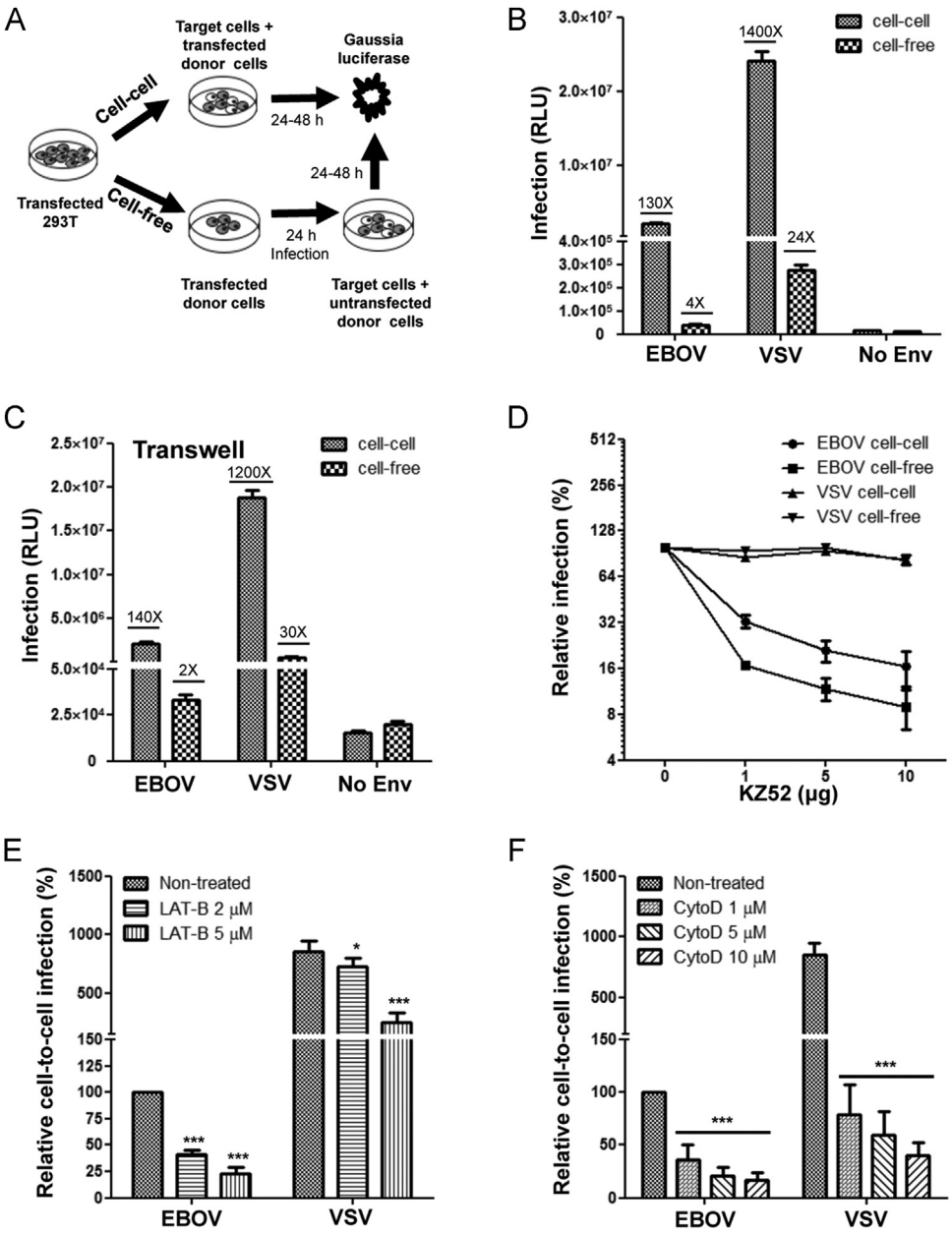

Fig. 1. EBOV GP mediates cell-to-cell infection of retroviral pseudotypes. (A) Schematic representation of cell-to-cell vs. cell-free infections. See details in Methods and Results. (B) Comparisons between cell-to-cell and cell-free infections mediated by EBOV GP and VSV-G. Results shown are averages of three independent experiments measured 24 and 48 h after co-culture. "No Env" indicates the background Gluc activity derived from co-culture of 293T donor cells transfected with "Tet-off" alone. The fold differences in Gluc activity above the corresponding "No Env" background are indicated. (C) Comparisons between cell-to-cell and cell-free infections in *Transwell* plates. The fold differences in Gluc activity above the corresponding "No Env" background are indicated. (D) Effect of KZ52 on cell-to-cell and cell-free infections. For cell-to-cell infection, KZ52 was added during co-culture. For cell-free infection, KZ52 was incubated with viral supernatants for 2 h at 37 °C prior to infection and maintained during infection. The efficiencies of cell-to-cell or cell-free infection of EBOV GP and VSV-G without KZ52 were set to 100%, respectively, and relative activities at different doses were calculated and plotted. (E) Effect of LAT-B on cell-to-cell infection mediated by EBOV GP or VSV-G. Two concentrations of LAT-B (i. e., 2 μM and 5 μM) were applied to co-culture, and Gluc activity was measured 24–48 h later. (F) Effect of CytoD on cell-to-cell infection mediated by EBOV GP or VSV-G. Three concentrations of CytoD were used during cell co-culture. Results are from at least three independent experiments. $^{*}p < 0.05$; $^{***}p < 0.001$.

of media after a 24–48 h co-culture (Fig. 1A, top). To control cell-free viral infection, we cultured the same numbers of transfected donor cells for the same period of time (24 h), and the collected supernatants were used to infect target 293FT/TRE-GLuc cells that had been pre-mixed with parental untransfected 293T cells; this procedure would ensure the same numbers of cells to be used for cell-free infection (Fig. 1A, bottom). Donor 293T cells expressing VSV-G or no envelope served as controls for cell-to-cell and cell-free infections.

Expression of EBOV GP in donor 293T cells led to a ~130-fold higher GLuc activity compared to the mock control ("No-Env") (Fig. 1B). In contrast, the cell-free infection was only 3–5-fold above the background (Fig. 1B), thus resulting in a 40-fold difference between cell-to-cell and cell-free infections. Similarly, the cell-to-cell infection efficiency mediated by VSV-G was much more higher than the cell-free infection, i. e, ~70-fold, although VSV-G generally exhibited much higher Gluc activities than EBOV GP in both cell-to-cell and cell-free infections (Fig. 1B). To confirm the greater cell-to-cell vs. cell-free infection mediated by EBOV GP, we next applied a *Transwell* culture system, where cell-to-cell infection was measured by co-culturing donor and target cells on the bottom of the Transwell plates; the cell-free infection was achieved by seeding the same number of donor cells on the top and target cells on the bottom, allowing cell-free virions to migrate through a 0.45 μM membrane. In this system, we observed a 70-fold and 40-fold difference between cell-to-cell and cell-free infection for EBOV and VSV, respectively (Fig. 1C).

We treated co-cultured cells with KZ52, a broadly neutralizing antibody against EBOV, and observed that while KZ52 inhibited cell-to-cell infection mediated by EBOV GP (Fig. 1D), its efficiency was consistently lower than that of cell-free infection; specificity was confirmed by the absence of an effect of KZ52 on VSV-G (Fig. 1D). We also treated co-cultured cells with inhibitors of actin polymerization, such as latrunculin B (LAT-B) and cytochalasin D (CytoD), which are known to block cell-to-cell transmission of other viruses (Dale et al., 2013), and we found that both drugs strongly inhibited, in a dose-dependent manner, cell-to-cell infection mediated by EBOV GP and VSV-G (about 5–10 fold, Fig. 1E and F). Interestingly, cell-free infection of EBOV was also inhibited by LAT-B and CytoD, but only ~2 fold; noticeably, the effect of CytoD on cell-free infection was not dose-dependent, suggesting possible cytotoxicity at higher doses (data not shown). Collectively, these results revealed that cell–cell contact can promote EBOV GP-mediated infection, a phenomenon that has recently been reported for HIV, hepatitis C virus (HCV) and influenza A virus (IAV) (Brimacombe et al., 2011; Catanese et al., 2013; Dale et al., 2013; Roberts et al., 2015).

Ebola virus-like particles (VLPs) bearing GP are efficiently transferred from cell to cell

We next evaluated if cell–cell contact can also promote EBOV GP-mediated transfer of VP40 VLPs by using VP40-Blam-based virion-fusion and VP40-GFP-based uptake assays. Upon a 2 h co-culture, approximately 8.5% of 293FT/tdTomato target cells exhibited beta-lactamase activity; the effect was inhibited by KZ52, LAT-B and CytoD (Fig. 2A and B). In contrast, no beta-lactamase activity was detected for cell-free infection performed in parallel (Fig. 2C, second bar in "EBOV" group). Similar results were also obtained for VSV-G, although the cell-to-cell transfer efficiency was higher for VSV-G and was not inhibited by KZ52 (Fig. 2A and B). Spinoculation of the same cell-free VLP stock to infect the same number of target cells resulted in ~4.7% of fusion-positive cells (FACS plots not shown), suggesting that the inability to detect beta-lactamase activity in the cell-free infection without spinoculation was not due to a lack of cell-free virions produced from the donor cells (Fig. 2C).

To directly measure VP40 protein transfer, we transfected 293T donor cells with VP40-GFP in the presence or absence of GP, and co-cultured the transfected cells with target 293FT/tdTomato cells. Similar to the results obtained for VP40-Blam, cell-to-cell transfer mediated by EBOV GP and VSV-G was detected after a 2 h co-incubation and the levels increased after 6 h (Fig. 2D and E). Of note, VP40-GFP alone ("No Env") exhibited some levels of transfer (possibly due to lipid-mediated non-specific transfer reported for EBOV), albeit at lower levels as compared to cells co-expressing GP or VSV-G (Fig. 2D and E). Once again, cell–cell transfer mediated by EBOV GP, but not by VSV-G or VP40 alone, was inhibited by KZ52, although LAT-B and CytoD both effectively blocked cell-to-cell transfer mediated of EBOV GP or VSV-G, but not by VP40 alone (Fig. 2D and E).

Cell-to-cell transfer mediated by EBOV GP can occur without retroviral Gag-Pol

Because of its high sensitivity, we used the Tet-off-based retroviral pseudotype system to interrogate the cellular and viral determinants required for cell-to-cell transfer mediated by EBOV GP. We first explored if EBOV GP alone is sufficient to mediate transfer of retroviral vector encoding Tet-off in the absence of MLV Gag-Pol, and found that, indeed, expression of EBOV GP in 293T donor cells (along with Tet-off but without MLV Gag-Pol) consistently led to a significant level of Gluc activity compared to the mock Tet-off control (~53 fold, compare bar 3 with bar 4; $p < 0.001$). Notably, inclusion of MLV Gag-Pol in donor cells further increased the Gluc activity only ~2-fold (compare bar 1 with bar 3; Fig. 3A). Similarly, expression of VSV-G in the absence of MLV Gag-Pol resulted in a marked increase in Gluc activity, again with less than a 2-fold enhancement by Gag-Pol in donor cells (Fig. 3A). To assess if EBOV GP-mediated transfer of Tet-off from cell to cell is due to a direct cell–cell fusion on the plasma membrane, we treated co-cultured cells with either neutral or low pH; however, no apparent differences between neutral and low pH in Gluc activity were found (Fig. 3B), nor was syncytia formation observed (data not shown). In contrast, Gluc activity was significantly increased (20-fold) for VSV-G upon a low pH pulse (Fig. 3B). To further confirm that the increased Gluc activity of EBOV GP was not due to direct cell–cell fusion on the plasma membrane, we expressed GP in target cells and Tet-off in donor cells; again, we observed no increase in Gluc activity compared to mock control regardless of pH treatment (Fig. 3C). The ability of this EBOV GP, which is tagged with a FLAG at the N-terminus and has no mucin domain, to mediate cell-to-cell transfer without MLV Gag-Pol was also confirmed in additional EBOV GP constructs: full length GP WT without any tag ("Native-GP") (Wool-Lewis and Bates, 1999), full length GP with an N-terminal FLAG tag ("F-GP"), and mucin-deleted GP without an N-terminal FLAG ("Δmuc-GP") (Fig. 3D).

A previous study has shown that Tet-off is present in exosomes or nanovesicles that can be secreted into culture media and transferred to adjacent cells (Mangeot et al., 2011). We therefore evaluated if the Gluc signal we detected might be due to secretion of exosomes containing GP and Tet-off from donor cells. We treated co-cultured cells with a chemical inhibitor of exosomal production, i.e., GW4869 (Trajkovic et al., 2008), and we observed that GW4869 indeed reduced the Gluc activity induced by EBOV GP or VSV-G in a dose-dependent manner (2, 5, and 10 μM) (Fig. 3E). Western blotting analysis showed that purified exosomes contained an abundant level of GP as well as the common exosome marker CD63 (Ramakrishnaiah et al., 2013; Thery et al., 2006) (Fig. 3F). We then treated target 293FT/Gluc cells with

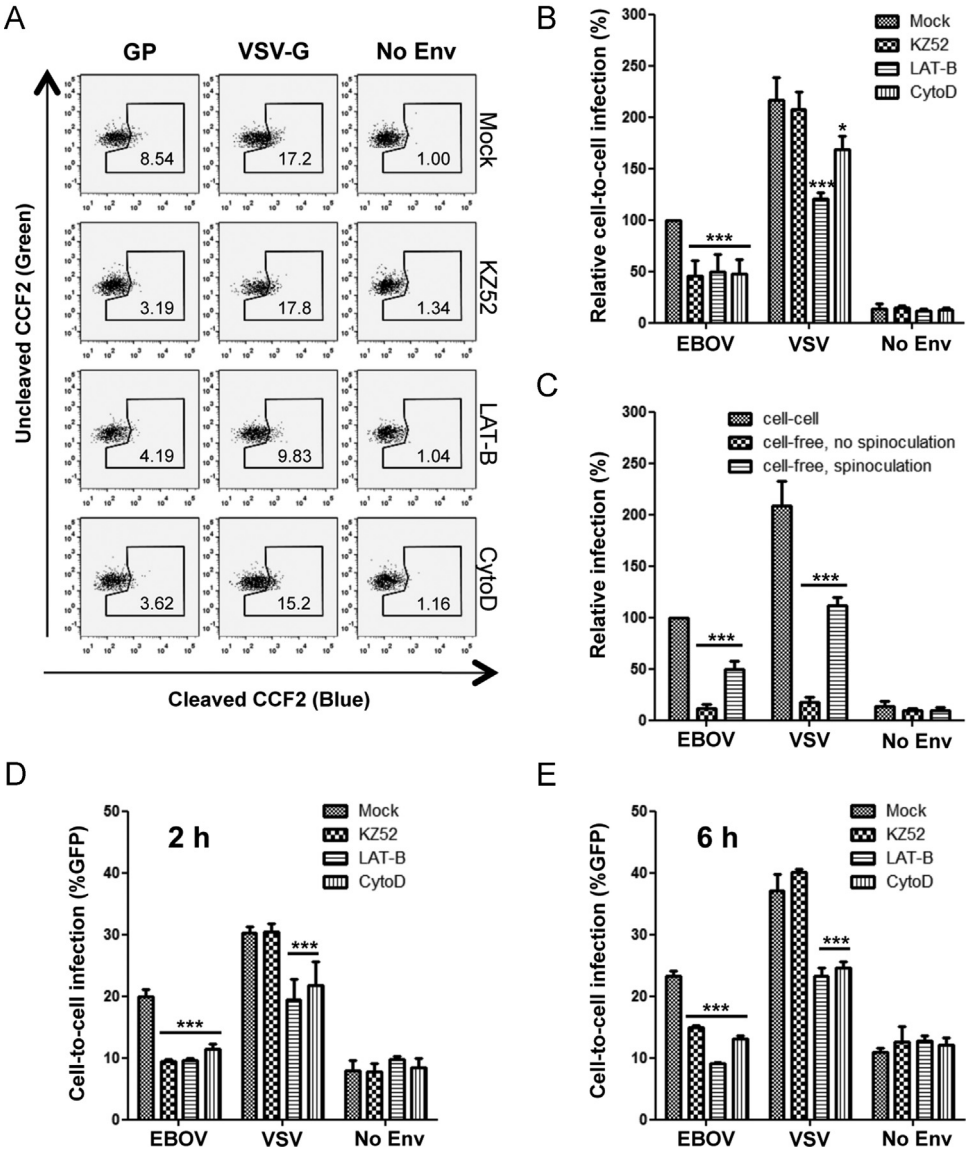

Fig. 2. EBOV virus-like particles (VLPs) are efficiently transmitted from cell to cell. 293T donor cells expressing VP40-Blam (A–C) or VP40-GFP (D and E) in the presence or absence of EBOV GP were co-cultured with 293FT/tdTomato target cells for different periods of time, and percentages of VP40-positive cells in target cells (red) were determined by a Blam-based fusion assay or by quantifying GFP signals using flow cytometry. (A) Cell-to-cell transfer of VP40-Blam in the presence of KZ52 or actin polymerization inhibitors (LAT-B and CytoD) was measured by a Blam-based virion-cell fusion assay. The cleaved CCF2 signals (blue) represent fusion-positive cells; the percentages are indicated inside the boxes. (B) Effect of KZ52, LAT-B, and CytoD on virion fusion following cell-to-cell transmission. The level of cell-to-cell infection with DMSO ("Mock") was set to 100% for plotting and comparison. (C) Summary of comparisons between cell-to-cell infection, cell-free infection without spinoculation, and cell-free infection with spinoculation, which are mediated by EBOV GP or VSV-G. Note that cell-free infection with spinoculation confirms the presence of virions in the supernatants of donor cells, which shows minimal levels of cell-free infection without spinoculation. (D and E) Cell-to-cell infection of VP40-GFP and the effect of KZ52 (20 μg/ml), LAT-B (1 μM), and CytoD (1 μM) after 2 h and 6 h of co-culture. Results are averages and standard deviations of 3–5 independent experiments. In all figures, $^{*}p < 0.05$; $^{**}p < 0.01$; $^{***}p < 0.001$.

purified exosomes, and observed an increased Gluc activity in target 293FT/gluc cells compared to exosome purified from mock cells not expressing GP (Fig. 3G). Taken together, these results suggest that exosomes secreted from donor cells contributed to the increased Gluc activity of EBOV GP (see Discussion).

Cleavage of EBOV GP by cathepsins is required for mediating cell-to-cell transfer

We next determined if GP-mediated enhancement of cell-to-cell transfer, even in the absence of a retroviral core, requires some of the essential factors known to be necessary for EBOV infection. Cleavage of EBOV GP by cathepsins B and L is required for EBOV infection, possibly by priming conformational changes of GP1 needed for receptor binding prior to membrane fusion (Chandran et al., 2005; Dube et al., 2009; Kaletsky et al., 2007; Schornberg et al., 2006; Wong et al., 2010). We applied a panel of protease inhibitors, including cathepsins B and L (referred to as CatB and CatL hereafter), and evaluated their effects on EBOV GP-mediated Tet-off transfer from donor cell to target cell. As shown in Fig. 4A, the pan-spectrum protease inhibitor leupeptin, the pan-cysteine cathepsin inhibitor E64d, as well as the CatB specific inhibitor CA074 all greatly inhibited Tet-off transfer mediated by EBOV ($p < 0.001$). In sharp contrast, none of these inhibitors had any effect on IAV (Fig. 4A). The reductions in EBOV GP-mediated cell-to-cell transfer caused by E64d and CA074 were dose dependent, with roughly comparable efficiencies (Fig. 4B; $p < 0.01$ or 0.001). We also treated co-cultured cells with cathepsin L inhibitor III, which inhibited EBOV GP-mediated but not IAV HA-mediated cell-to-cell transfer (Fig. 4C).

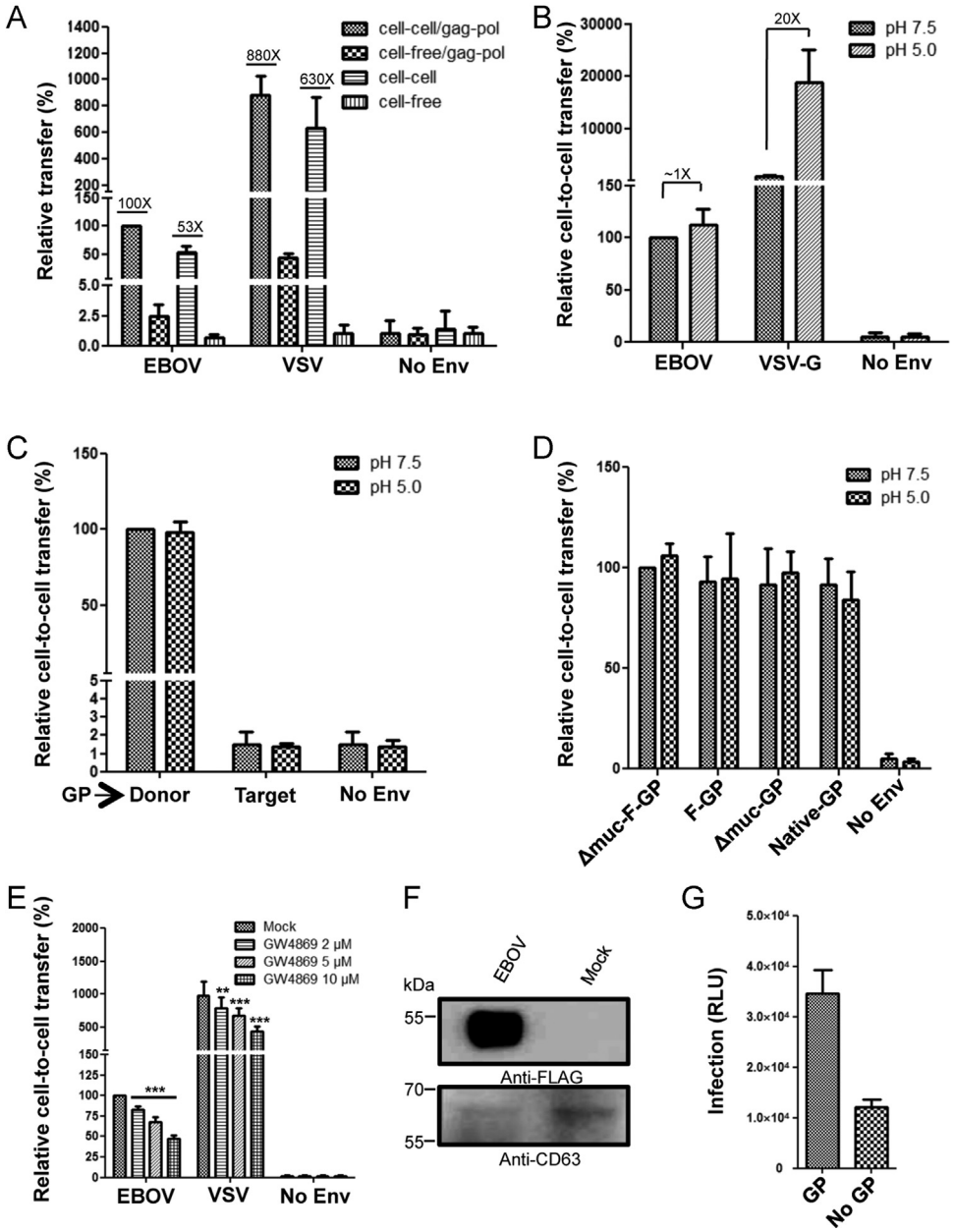

Fig. 3. Cell-to-cell transfer of retroviral pseudovirions occurs in the absence of MLV Gag-Pol and involves exosomes. (A) Comparisons of cell-to-cell and cell-free infections in the presence or absence of MLV Gag-Pol. The fold differences in Gluc activity above the corresponding "No Env" background are indicated. Note that a ~2-fold increase in cell-to-cell transfer resulted from the presence of MLV Gag-Pol. (B) Low pH treatment increases cell-to-cell transfer mediated by VSV-G but not by EBOV GP. A pH 5.0 pulse was applied after a 2 h co-culture, and Gluc activity was measured at 24 and 48 h, respectively. The fold differences in Gluc activity between neutral and low pH are indicated. (C) Expression of EBOV GP (and Tet-off) in donor cells, but not in target cells, led to efficient cell-to-cell transfer. (D) The ability of EBOV GP to mediate cell-to-cell transfer is confirmed by testing different versions of EBOV GP constructs. Δmuc-F-GP: a mucin-deleted GP with a FLAG tag at the N-terminus, which is mainly used in this study; F-GP: a full length GP with the FLAG tag at the N-terminus; Δmuc-GP: a mucin-deleted GP without any tag; Native-GP: a full length GP without any tag. Relative cell-to-cell transmission of EBOV GP was calculated by setting that of Δmuc-F-GP to 100%. (E) Effect of the exosome inhibitor GW4869 on cell-to-cell transfer. Different concentrations of GW4869 were tested. (F) Western blotting reveals the presence of EBOV GP (anti-FLAG) in concentrated exosomes. CD63 serves as a marker of exosomes. (G) Infection of 293FT/Gluc target cells with purified exosomes containing GP results in increased Gluc activity. Absolute Gluc read-outs are shown. In all figures, $^{**}p < 0.01$; $^{***}p < 0.001$.

To distinguish if the effects of these protease inhibitors were on donor cells or target cells, we treated donor cells with leupeptin for 24 h before and during co-culture, or treated both donor and target cells during co-culture. Treatment of donor cells alone had no effect on Gluc activity; however, treatment of target cells alone or in combination with donor cells significantly decreased Gluc activity (Fig. 4D). These results indicate that cathepsin activity in target cells, rather than in donor cells, is crucial for GP to mediate cell-to-cell transfer.

Given that the protease activities of CatB and CatL are dependent on the acidification of late endosomes and lysosomes (Schornberg et al., 2006), we next treated co-cultured cells with NH_4Cl, a lysosomotropic agent, which neutralizes the acidic pH of late endosomes and lysosomes and thereby blocks EBOV infection (Takada et al., 1997). Cell-to-cell transfer mediated by EBOV GP or VSV-G was both strongly inhibited by NH_4Cl in a dose-dependent manner ($p < 0.001$) (Fig. 4E). These results together demonstrated that pH-dependent cathepsin activity is required for cell-to-cell transfer, a property that is in line with cell-free EBOV entry.

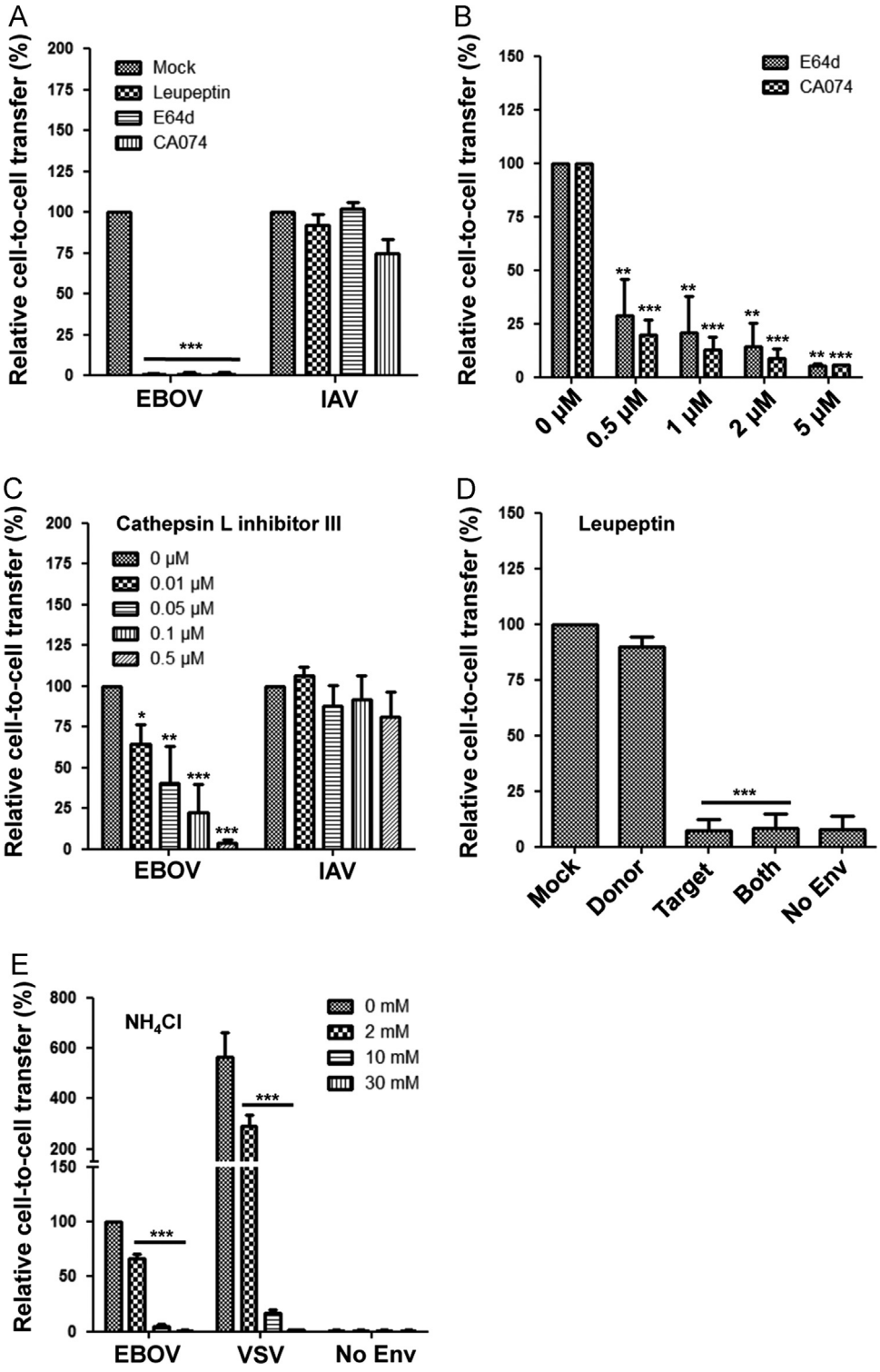

Fig. 4. Cellular cathepsin activity is essential for cell-to-cell transfer of EBOV GP. (A) Effects of leupeptin, CA074, and E64d on cell-to-cell transfer of EBOV GP and IAV HA. Co-cultured cells were treated with 50 μM leupeptin, 5 μM E64d, or 5 μM CA074 throughout the assay, and Gluc activity was measured 24–48 h after co-culture. (B and C) Effects of different doses of E64d, CA074, or CatL III inhibitor on cell-to-cell transfer mediated by EBOV GP or IAV HA. For comparison, cell-to-cell transfer efficiencies of EBOV GP and IAV HA in the absence of inhibitors are set to 100%, respectively. (D) Effects of leupeptin added to donor cell, target cells, and both on cell-to-cell transfer mediated by EBOV GP. (E) Effects of NH_4Cl on cell-to-cell transfer mediated by EBOV GP and VSV-G. Unless otherwise specified, results represent the averages ± standard deviations of at least three independent experiments. $^{*}p < 0.05$; $^{**}p < 0.01$; $^{***}p < 0.001$.

NPC1 and TIM-1 promote cell-to-cell transfer mediated by EBOV GP

Several cellular factors have recently been reported to function as receptors or cofactors for EBOV, with NPC1 and TIM-1 being the most prominent (Carette et al., 2011; Côté et al., 2011; Kondratowicz et al., 2011; Miller et al., 2012). We evaluated the possible roles of these two cellular factors in EBOV GP-mediated infection by cell–cell contact. To facilitate our analyses, we established target 293FT/Gluc cell lines stably expressing full length NPC1, or the NPC1 domain C without the cytoplasmic tail (gift of Kartik Chandran referred to as NPC1 CT

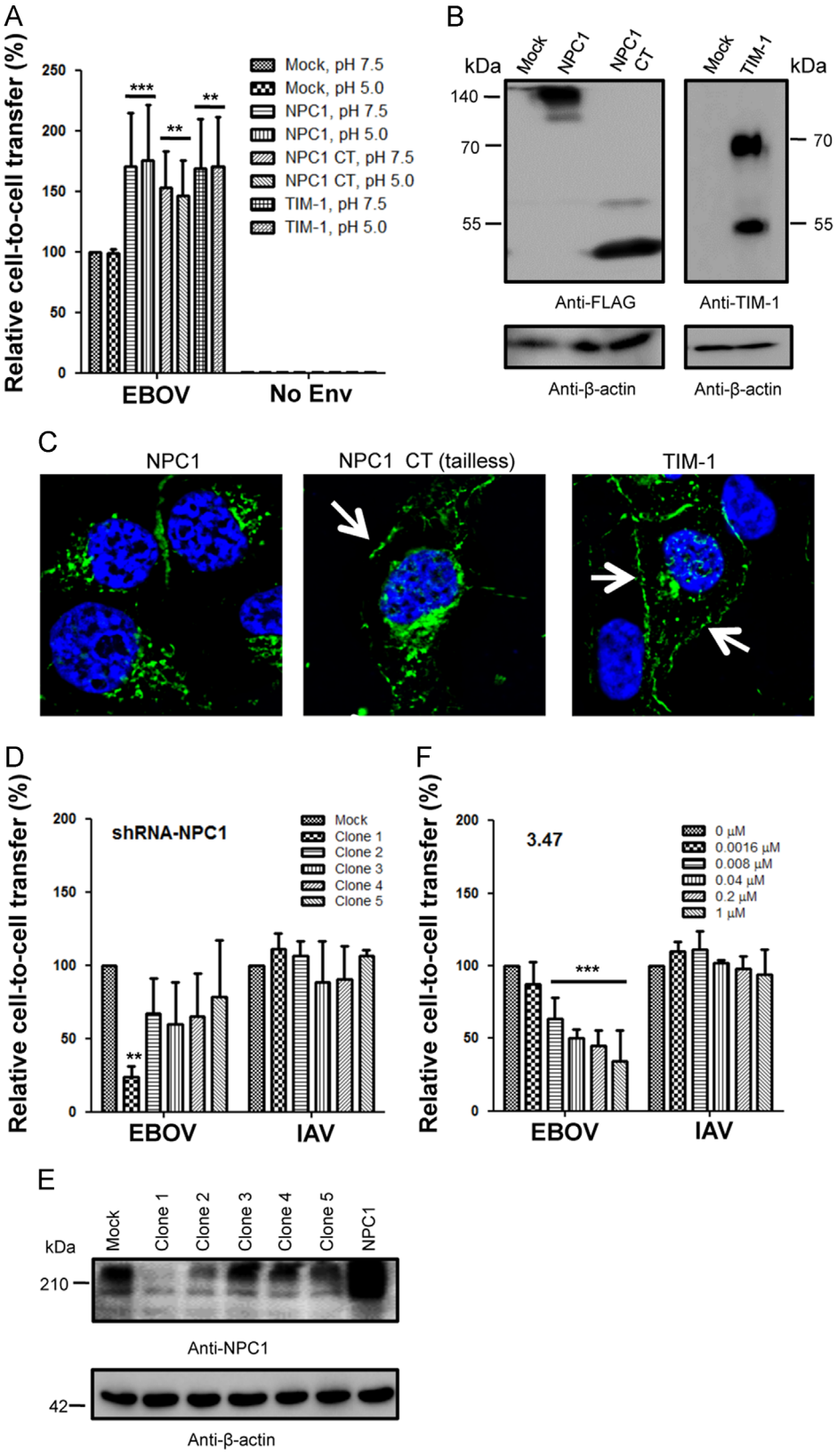

Fig. 5. Overexpression of NPC1 or TIM-1 increases cell-to-cell transfer mediated by EBOV GP. (A) Cell-to-cell transfer by EBOV GP was examined in parental 293FT/Gluc (Mock, set to 100%) or 293FT/Gluc cells overexpressing full length NPC1 (NPC1) or the NPC1 domain C with the cytoplasmic tail truncated (NPC1 CT) at neutral or low pH. (B) Western blotting analysis of the expression of NPC1 and NPC1 CT using anti-FLAG. β-actin served as the loading control. (C) Immunostaining of 293FT/Gluc cells overexpressing NPC1 and NPC1 CT (tailless). Cells were permeabilized and stained with an anti-FLAG antibody, and the fluorescence signal was visualized and analyzed by a 3D deconvoluted fluorescence microscope (Leica). Arrows indicate fluorescence signals on the cell surface. (D) Relative cell-to-cell transfer mediated by EBOV GP and IAV HA examined in target cells stably expressing lentiviral vectors encoding NPC1 shRNA. Five stable cell lines expressing different clones of NPC1 shRNAs were tested, with clone 1 (Sigma #5428) consistently exhibiting significant reduction in cell-to-cell transfer. The cell-to-cell transfer mediated by EBOV GP in parental 293FT/Gluc was set to 100% for comparison. (E) Western blotting analysis of NPC1 in 293FT/Gluc cells expressing NPC1 shRNA. An anti-NPC1 antibody was used for probing NPC1 expression; β-actin served as the loading control. (F) Effects of 3.47 on cell-to-cell transfer mediated by EBOV GP and IAV HA. Indicated concentrations of 3.47 were added to the co-culture media for 24–48 h before Gluc activity was measured. In all cases, $^{**}p < 0.01$; $^{***}p < 0.001$.

hereafter) (Miller et al., 2012), or human TIM-1 (Li et al., 2014). We found that full-length NPC1, NPC1 CT, as well as TIM-1 all enhanced cell-to-cell transfer mediated by EBOV GP ($p < 0.01$ or 0.001), with no apparent differences between neutral and low pH (Fig. 5A). The expression of these cellular proteins in target cells was confirmed by Western blotting (Fig. 5B). Immunofluorescence staining revealed that TIM-1 was predominantly expressed on the cell surface, as expected; NPC1 CT was also detectable on the cell surface, similar to a previous report (Miller et al., 2012), but with much less fluorescence intensity than found for TIM-1 (Fig. 5C). The full length NPC1 protein was primarily expressed in intracellular vesicles (Fig. 5C).

We next knocked down NPC1 in 293FT/Gluc target cells by transducing cells with shRNA lentiviral vectors, and examined their effects on cell-to-cell transfer mediated by EBOV GP. Among the 5 shRNA clones tested, one clone (clone 1, Sigma #5428) consistently exhibited the strongest inhibition of cell-to-cell transfer

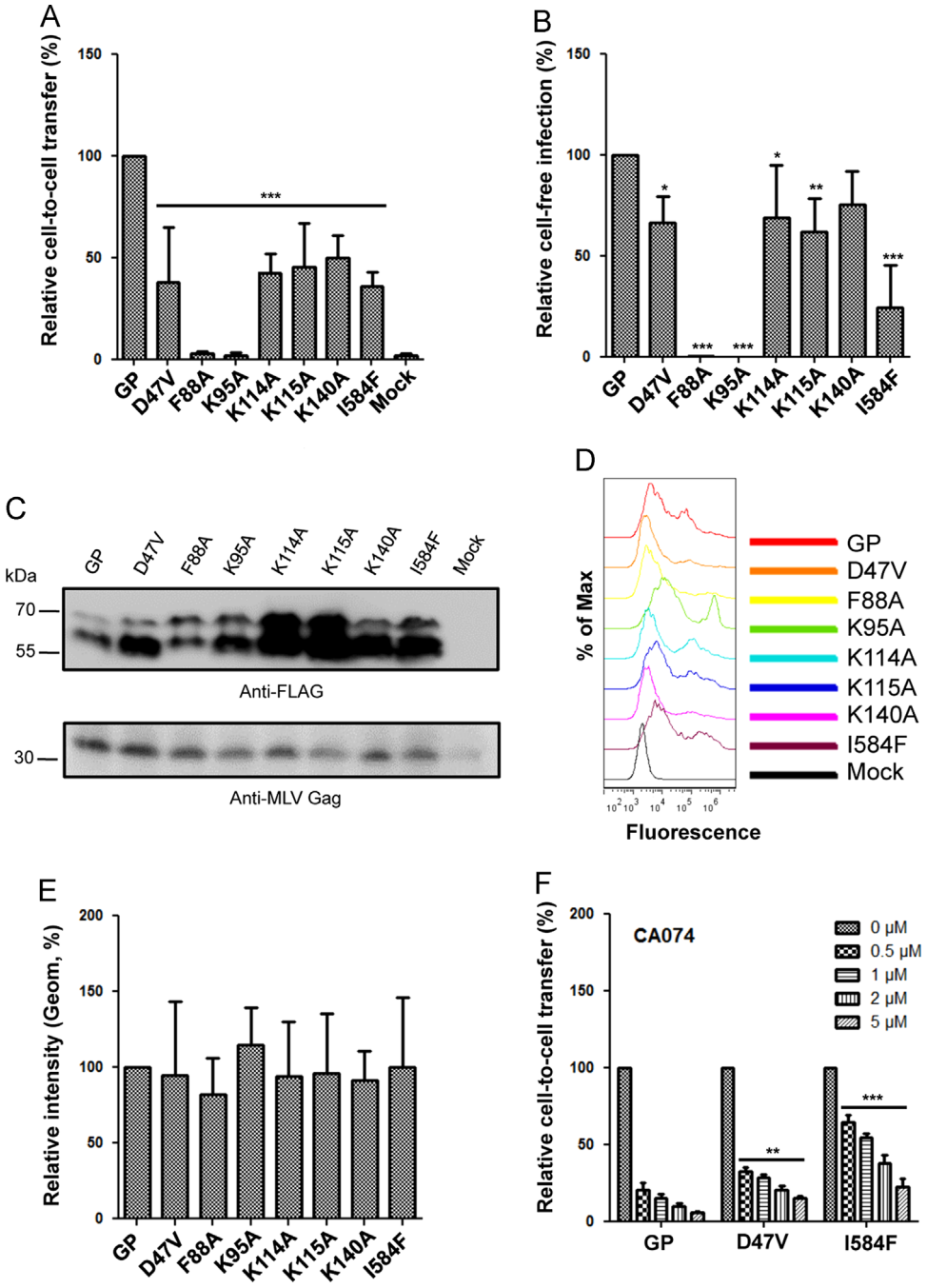

Fig. 6. Cell-to-cell transfer mediated by EBOV GP requires receptor-binding. (A) Comparisons of cell-to-cell transfer by EBOV GP mutants. The transfer efficiency of parental GP was set to 100%. (B) Relative cell-free infection of EBOV GP mutants in HTX cells. Note that in this case, pseudovirions were generated from 293GP/LAPSN cells (normal transfection scale in 6-well plate) and used to infect HTX; AP positive foci in HTX cells were counted 72 h post-infection. The infectivity of parental GP was set to 100% for comparison. (C) Western blotting analysis of EBOV GP mutants using an anti-FLAG antibody. β-actin served as the loading control. (D and E) Flow cytometry analysis of the surface expression of parental EBOV GP and mutants. 293T cells were transiently transfected with plasmids encoding EBOV GPs and stained using an anti-FLAG antibody. Representative flow cytometry profiles from one typical experiment are shown (D). Quantification of the fluorescence intensities of EBOV GPs (E). The geometric mean (Geom) of each GP mutant was compared to that of parental GP, the latter of which was set to 100%. Results were summarized from three independent experiments. (F) Differential sensitivities of EBOV GP-mediated cell-to-cell transfer to the CatB inhibitor, CA074. Cell-to-cell transfer mediated by each GP mutant without being treated with CA074 was set to 100%. The p values indicate results of comparisons between D47V or I584F and parental GP at each equivalent concentration of CA074. $^{*}p < 0.05$; $^{**}p < 0.01$; $^{***}p < 0.001$.

mediated by EBOV GP ($p < 0.01$ or 0.001) (Fig. 5D). The level of NPC1 expression in 293FT/Gluc target cells expressing this shRNA clone was most reduced compared to cells expressing other shRNAs and mock control (Fig. 5E). We also treated co-cultured cell with 3.47, a small molecule inhibitor that specifically blocks EBOV GP to bind to NPC1, and found that it significantly inhibited EBOV GP-mediated cell-to-cell transfer ($p < 0.001$) in a dose-dependent manner (Fig. 5F). Knockdown of NPC1 or treatment of cells with 3.47 showed no effect on IAV HA-mediated cell-to-cell transfer (Fig. 5D and E). Altogether, these results demonstrate that endogenous NPC1 does play a role in EBOV GP-mediated cell-to-cell transfer, consistent with its reported role in EBOV cell-free infection (Carette et al., 2011; Côté et al., 2011; Miller et al., 2012).

The receptor-binding property of EBOV GP is critical for cell-to-cell transfer

We further investigated the role of receptor binding in EBOV GP mediated infection by cell-cell contact by making a series of GP mutants in GP1—F88A, K95A, K114A, K115A and K140A—which have been previously shown to impair the binding of EBOV GP to putative receptors and NPC1 (Brindley et al., 2007; Dube et al., 2009; Lee et al., 2008; Manicassamy et al., 2005; Miller et al., 2012; Ou et al., 2010; Wang et al., 2011; Watanabe et al., 2000). We found that all of these mutants exhibited significantly decreased cell-to-cell transfer efficiency; F88A and K95A had the most dramatic phenotype, showing an almost complete loss in Tet-off transfer ($p < 0.001$) (Fig. 6A). Consistent with the cell-to-cell transfer data, the cell-free infection of these mutants encoding alkaline phosphatase (AP), especially F88A and K95A, was also greatly reduced compared to the parental GP, albeit to different extents ($p < 0.05$, 0.01 or 0.001) (Fig. 6B). Western blotting analysis showed that all these GP mutants were expressed and processed into GP1 and GP2 in viral producer cells, although to somewhat different levels or efficiencies (Fig. 6C). While the relatively low level of expression of F88A could have contributed to its low cell-to-cell transmission activity, most mutants, including K95A, were well expressed in transfected cells, including on the cell surface (Fig. 6D and E), indicating that the reduced cell-to-cell and cell-free infection efficiencies observed for most of these GP mutants likely reflect their intrinsic low receptor binding and/or fusion potential.

We next evaluated two additional GP mutants, D47A and I584F, which have been recently shown to mediate EBOV entry in a somewhat CatB-independent manner (Misasi et al., 2012; Wong et al., 2010). Indeed, adding the CatB inhibitor CA074 to co-cultured cells did not reduce cell-to-cell transfer for either mutant, especially I584F, to the same extent as for the parental GP at all concentrations tested ($p < 0.01$ or 0.001) (Fig. 6F). The relative insensitivity of mutants GP1 D47A and GP2 I584F to CA074 is consistent with their relative independence from CatB-mediated priming in membrane fusion and EBOV entry.

Co-culturing epithelial cells and macrophages promotes spread of recombinant VSV (rVSV) bearing EBOV GP

The above data suggest that EBOV GP can efficiently mediate transfer of VP40 or Tet-off from cell to cell. We next determined if this could also occur in a replication-competent viral system, especially in monocytes and macrophages, which are the primary targets of EBOV infection in vivo. For this purpose, we employed a replication-competent rVSV-GFP system that expresses EBOV GP (rVSV-GFP-GP). We first infected 293T donor cells with appropriate doses of rVSV-GFP-GP so that optimal numbers of GFP positive (green) donor cells would be produced. We then co-cultured these donor cells with target 293FT/Gluc cells that were pre-labeled with CMTMR, and cell-to-cell infection was measured by gating the CMTMR-positive cells for GFP signals. In parallel, we also determined cell-free infection by infecting the same CMTMR-labeled target cells with rVSV-GFP-GP produced from donor cells (see Methods for details).

After 2 h of co-culture, the infection rate of rVSV-GFP-GP, which likely reflected a combination of cell-to-cell and cell-free infection, was low (i.e., 0.86%). Infection was, however, significantly increased at 6 h (9.9%) and 12 h (47.1%) (Fig. 7A). In contrast, cell-free infection of rVSV-GFP-GP was virtually undetectable before 6 h following co-culture (0.708%), and only became quite apparent after 12 h (4.58%); this was 10-fold lower than infection via cell-cell contact. By treating the co-cultured cells with KZ52, LAT-B, or CytoD, as we had done for retroviral pseudoviral and VLP systems, we observed that rVSV-GFP-GP infection via cell–cell contact was strongly inhibited by all three agents (Fig. 7B). Of note, cell-free infection of rVSV-GFP-GP was also affected by LAT-B and Cyto-D, consistent with a previous report (Yonezawa et al., 2005).

We then performed a similar cell-to-cell infection assay by using THP-1 or THP-1 cells treated with PMA, which served as either donor or target cells; PMA is known to differentiate THP-1 monocytes to macrophages. In both cases, the rVSV-GFP-GP infection efficiency mediated in co-cultured cells was much greater than was cell-free infection (Fig. 7C and D). Notably, rVSV-GFP-GP transfer from PMA-treated THP-1 cells to 293FT/Gluc cells was about 10-fold more efficient than transmission from parental THP-1 cells to 293FT/Gluc (data not shown), which likely reflects the low infection capability of donor THP-1 cells by rVSV-GFP-GP as compared to PMA-treated THP-1 cells. However, there was no significant difference between PMA-treated or untreated THP-1 cells when they served as target cells (compare bar 1 and bar 3, $p > 0.05$; Fig. 7E). Similar to the results shown for 293T-to-293FT transfer, both cell-to-cell infection and cell-free infection of rVSV-GFP-GP were strongly inhibited by KZ52, LAT-B and CytoD (Fig. 7C and D).

To confirm the results of cell-to-cell spread infection of rVSV-GFP-GP between 293T and 293FT cells, we applied a viscous 1% methylcellulose solution to co-cultured 293T and 293FT/Tomato cells; in parallel, this solution was also applied to cell-free viral infection. Previously, methylcellulose has been used to distinguish between cell-cell and cell-free viral infection (Jin et al., 2009). As shown in Fig. 7F and G, methylcellulose almost completely blocked the cell-free infection of rVSV-GFP-GP, yet had no apparent effect on cell-to-cell infection. Taking all above results together, we conclude that coculturing monocytes/macrophages and epithelial cells enhances spread of replication-competent rVSV-GFP-GP in vitro.

Discussion

Using retroviral pseudotypes, EBOV VP40-based VLPs, as well as rVSVs encoding GP, we demonstrate in this work that cell–cell contact promotes EBOV GP-mediated infection. Interestingly, we found that the EBOV GP protein alone, even in the absence of the retroviral Gag-Pol, is sufficient to transfer Tet-off from cell to cell, and that the key molecules involved in cell-to-cell transfer parallel that of authentic EBOV infection. We further showed that the cellular cathepsins B/L and NPC1 are essential for cell-to-cell transfer to occur. We ruled out the possibility that cell–cell fusion on the plasma membrane is responsible for the increased Gluc activity by separately expressing EBOV GP in target cells and Tet-off in donor cells, with no Gluc activity detected.

Several lines of evidence support the conclusion that cell-to-cell transfer of Tet-off from donor cells to target cells mediated by EBOV GP is specific and not due to experimental artifacts. First, the increase in Gluc activity is only detected in cells co-expressing

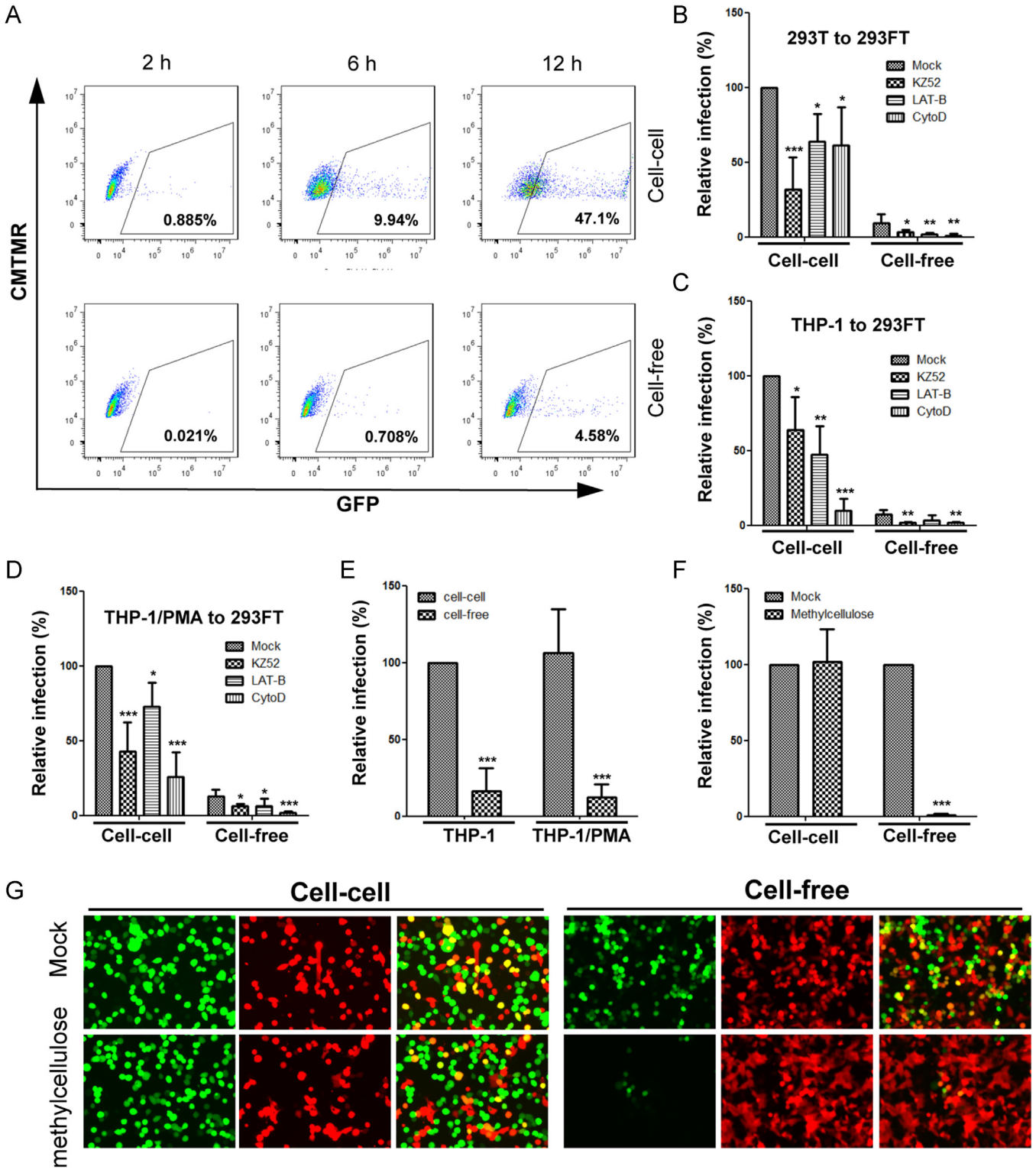

Fig. 7. Cell-to-cell transmission occurs in epithelial cells and macrophages for replication-competent rVSV encoding EBOV GP. (A–D) Cell-to-cell transmission was performed by co-culturing donor cells (293T, THP-1 or PMA-treated THP-1 cells) infected with appropriate amounts of rVSV-GFP encoding EBOV GP (green) and target 293FT cells that were pre-labeled with CMTMR (red). The efficiency of cell-to-cell transmission was determined by gating the GFP positive cell population in the CMTMR-labeled cells using flow cytometry. (A) Representative flow cytometry files show the infection rates of rVSV-GFP-EBOV GP via cell-to-cell transmission or cell-free infection at 2, 6 and 12 h following co-culture. (B) Summary of the transmission of rVSV-GFP encoding EBOV GP from 293T to 293FT cells in comparison with that of cell-free infection; the effects of KZ52, LAT-B, and CytoD on these two modes of infection are also shown. (C and D) Transmission of rVSV-GFP encoding EBOV GP from THP-1 cells or PMA-treated THP-1 (macrophages) to 293FT cells. In all cases, 20 μg/ml of KZ52, 1 μM of LAT-B, or 1 μM of CytoD were used to treat co-cultured cells. Results shown are from at least three independent experiments performed in duplicate. (E) Transmission of rVSV-GFP encoding EBOV GP from 293FT cells to THP-1 cells or THP-1 cells treated with PMA (macrophages). (F) Effects of methylcellulose on cell-to-cell transmission or cell-free infection of rVSV-GFP encoding EBOV GP. 293T cells were infected with appropriate amounts of rVSV expressing EBOV GP; 24 h post-infection, the infected 293T cells were co-cultured with 293FT/tdTomato cells at a 1:3 ratio in the presence or absence of 1% methylcellulose. GFP signals in the Tomato-positive cell populations were analyzed by flow cytometry. For cell-free virus infection, 293FT/tdTomato cells were directly infected with appropriate amounts of rVSV expressing EBOV GP in the presence or absence of 1% methylcellulose. (G) Representative images showing cell-to-cell transmission or cell-free infection of rVSV-GFP encoding EBOV GP in the presence or absence of methylcellulose (mock). Note that the rVSV-GFP-GP viral stocks used for cell-free infection here were not from the same donor cells used for cell-to-cell infection. Images shown were taken after 18–24 h after infection. In all cases, results were from at least three independent experiments. $^{*}p < 0.05$; $^{**}p < 0.01$; $^{***}p < 0.001$.

viral glycoprotein GP; it is not detected for cells expressing Tet-off alone. Second, the increased Gluc signal in the culture media of GP-expressing cells, but not that of VSV-G-expressing cells, is diminished by KZ52, a broadly neutralizing antibody against EBOV GP, as well as by 3.47, a small molecule inhibitor that specifically blocks EBOV GP from binding to its receptor NPC1. Third, EBOV GP mutants deficient for NPC1 binding or infection exhibit decreased activities of cell-to-cell transfer efficiency. In addition, we tested an EBOV GP mutant engineered to harbor a furin-recognizing sequence in place of the putative cathepsin L cleavage site and found that this GP exhibits significantly increased cell-to-cell transfer efficiency (data not shown). It is noteworthy that other viral glycoproteins, such as VSV-G and IAV HA, can also efficiently mediate cell-to-cell transfer of Tet-off at neutral pH. However, the Gluc activities induced by these two viral fusion proteins are dramatically enhanced by an extracellular low pH pulse, indicating that cell–cell fusion at the plasma membrane can contribute to cell-to-cell transfer, although this is not the case for EBOV, nor for VSV-G and IAV HA, all of which require low pH directly or indirectly for fusion. Because no infectious EBOV virions or virus-like particles are involved in this very sensitive Tet-off-based cell-to-cell infection assay, we suggest that this system could be extremely useful for study of highly contagious BL4 agents such as EBOV and Hanta virus, including screens for potential entry inhibitors.

What are the possible mechanisms of the enhancement of EBOV GP-mediated cell-to-cell infection compared to cell-free infection? One obvious possibility is that cell–cell contact can increase the local concentrations of retroviral pseudovirions, EBOV VLPs, and rVSV-GP, resulting in relatively high MOIs that enhanced infection and spread. In contrast, viral particles in the cell-free infection system may be relatively unstable, or more susceptible to inactivation by serum and other culture conditions. Evidence supporting this scenario is that spinoculation of cell-free virions produced from donor cells did increase cell-free infection efficiency. Additionally, we provide data showing that exosomes, which may or may not be concentrated in the cell–cell contact area, are enriched with EBOV GP, and that inhibition of exosome release by a chemical inhibitor GW4869 led to decreased Tet-off transfer from cell to cell. Indeed, exosomes have recently been shown to play roles in viral cell-to-cell transmission and pathogenesis, although the underlying mechanism remains murky (Madison and Okeoma, 2015); more work is needed to dissect the exact roles of exosomes in EBOV infection. It is formally possible that different forms of EBOV GP, including full-length GP as well as secreted GP (sGP), may function through exosomes that modulate EBOV spread in a VP40-indepenent fashion.

Our study strongly suggests, though does not definitely prove, that EBOV GP promotes viral cell-to-cell transmission in addition to mediating cell-free infection; not surprisingly, both modes of infection require cathepsin and NPC1. Strong similarities between cell-to-cell and cell-free infection, including sensitivities to the neutralizing antibodies, have also been demonstrated for HIV (Agosto et al., 2014). It is thus possible that EBOV GP may associate with some cell surface molecules, including TIM-1 and DC-SIGN, thereby creating a structure known as virological synapse (VS) to facilitate cell-to-cell transmission. It is also possible that EBOV particles may travel from donor cell to target cell through nanotubular or related structures. Hence, detailed analyses of EBOV infection using high-resolution live-cell imaging would be informative to address these possibilities. Ultimately, we will need to address if authentic live EBOV, or EBOV derived from reverse genetics systems (Hoenen and Feldmann, 2014b), can spread via cell–cell contact in humans and animal infections as well as their implications for viral pathogenesis and antiviral therapy (Qiu et al., 2014; Warren et al., 2014).

Materials and methods

DNA constructs and plasmids

The native full-length EBOV GP construct was originally provided by Gary Kobinger (National Microbiology Laboratory, Winnipeg, Canada). The mucin-deleted EBOV GP (pcDNA- Δmuc-GP) was originally provided by David Sanders (Purdue University). The N-terminal FLAG-tagged full length EBOV GP construct (F-GP) was made by replacing the signal peptide of GP with that of preprotrypsin followed by a FLAG sequence (inserted between the signal peptide and mature GP); this F-GP was subcloned into the backbone of pCIneo (Promega). The N-terminal FLAG-tagged GP present in pCIneo-F-GP was subcloned into the mucin-deleted pcDNA-Δmuc-GP construct, resulting in Δmuc-F-GP, which was primarily used in this study. All EBOV GP mutants were generated by overlapping PCR-based mutagenesis using pcDNA-F-Δmuc construct as the template. All constructs were confirmed by DNA sequencing.

The pQCXIP-Tet-off construct was provided by Marc Johnson (University of Missouri) (Janaka et al., 2013). The 3 × FLAG-tagged NPC1 and NPC1 domain C proteins with the cytoplasmic tail deleted constructs (referred to as NPC1 CT in this work) were from Kartik Chandran (Albert Einstein College of Medicine) (Miller et al., 2012). VP40 was provided by Yoshihiro Kawaoka (University of Wisconsin, Madison), VP40-Blam was provided by Lijun Rong (University of Illinois, Chicago) and VP40-GFP was provided by Kartik Chandran. The influenza HA and NA constructs were offered by Gary Nabel (Vaccine Research Center, NIH).

Cell lines and reagents

293T, 293GP/LAPSN (expressing MLV Gag-Pol and transfer vector encoding alkaline phosphatase) and HTX (a subclone of HT1080) have been previously described (Côté et al., 2008). THP-1 cells were obtained from ATCC. The 293FT/Gluc cell line that stably expresses Gluc was provided by Marc Johnson (Janaka et al., 2013). The 293FT/Gluc cell lines stably expressing NPC1or NPC1 CT or TIM-1 were generated by transducing 293FT/Gluc cells with pBabe (for NPC1 and NPC1 CT) or with a pQCXIP (for TIM-1) retroviral vector expressing the individual proteins, followed by puromycin selection (Sigma, 2 μg/ml). All cells were grown in Dulbecco's modified Eagle's (DMEM) medium, supplemented with 0.5% penicillin/streptomycin plus 10% fetal bovine serum (FBS).

The human KZ52 antibody was provided by Dennis Burton and Erica Saphire (The Scripps Research Institute) (Lee et al., 2008; Parren et al., 2002). The rabbit antibody against EBOV GP1 and 3.47 were obtained from James Cunningham (Harvard Medical School) (Côté et al., 2011). The anti-NPC1 antibody was purchased from Abcam (Cambridge, MA). The anti-TIM-1 antibody was purchased from R&D Systems. The anti-CD63 antibody was purchased from Invitrogen (Carlsbad, CA). The anti-MLV Gag antibody was purified from R187 hybrioma cell line (ATCC). Leupeptin, E64d, CA074, and cathepsin L inhibitor III (Z-Phe-Tyr(t-Bu)-diazomethylketone, also known as Z-FY(t-Bu)-DMK) were all purchased from EMD Millipore (Billerica, MA). Ammonium chloride (NH_4Cl), 12-O-Tetradecanoylphorbol 13-acetate (PMA), methylcellulose, GW4869, shRNA lentiviral vectors targeting NPC1, anti-FLAG antibody, anti-β-actin antibody, and secondary anti-mouse immunoglobulin G conjugated to FITC or HRP were purchased from Sigma (St Louis, MO). The *Gaussia* luciferase activity was measured by following the manufacturer's instructions (Promega, Madison, WI) with minor modifications.

Cell-to-cell infection

For the retroviral vector-based system, 293T cells were seeded onto six-well plates and transfected with 1 μg pQCXIP-Tet-off vector, 1 μg MLV Gag-Pol and 0.5 μg of plasmids encoding EBOV GP, IAV HA or VSV-G. Alternatively, MLV Gag-Pol was omitted in the transfection. The next day, 2×10^5 of the transfected 293T donor cells were thoroughly washed and trypsinized in order to remove bound virus and residual plasmid DNA, followed by co-culturing with 4×10^5 293FT/Gluc target cells or derivatives in 24-well plates for 24–48 h. Inhibitors were added during co-culture unless otherwise specified. For *Transwell* settings, cell-to-cell infections were determined by co-culturing donor and target cells on the bottom (without insert) and cell-free infection was measured by seeding donor cells on the top well and target cells mixed with the same number of untransfected donor cells on the bottom. Approximately 2 μl of co-cultured media were assayed for Gluc activity in 10 μl buffer containing 10 μM coelenterazine in 0.1 M Tris, pH 7.4 and 0.3 M sodium ascorbate. In all experiments, 293T donor cells transfected with pQCXIP-Tet-off alone were co-cultured with target cells to serve as background control.

For the VP40-based VLP assay, we transfected 293T cells with VP40-Blam or VP40-GFP in the presence or absence of EBOV GP. The transfected cells were co-cultured with 293FT/tdTomato cells, and cell-to-cell transfer efficiency was determined by measuring virus uptake using a Blam-based virion-fusion assay (Tscherne and Garcia-Sastre, 2011) or by detecting a GFP signal using flow cytometry. Inhibitors were added during co-culture if applicable.

For the rVSV-based assay, 293T, THP-1, or PMA-treated THP-1 cells were infected with appropriate amounts of rVSV-GFP expressing EBOV GP or VSV-G (kindly provided by Kartik Chandran), and the infected cells were co-cultured with CMTMR-labeled 293FT, THP-1, or THP-1 cells treated with PMA, or co-cultured with 293FT/tdTomato cells (red). If desirable, 1% methylcellulose was laid on top of co-cultured cells. Cell-to-cell infection was measured by flow cytometry by measuring the GFP signal in red-cell populations or visualized by fluorescence microscope. Inhibitors were applied during co-cultured as needed.

Cell-free infection

When counting donor cells for cell-to-cell infection, an equivalent number (2×10^5) of transfected or infected donor cells were seeded onto a new 6-well plate and cultured for the same time period as the duration of cell-to-cell infection. The total volumes of supernatants were harvested, and used to infect target cells that were mixed with un-transfected 293T cells; this ensured that cell numbers used for cell-to-cell and cell-free assays were absolutely comparable. If needed, spinoculation or 1% methylcellulose was applied during infection. The cell-free infectivity was determined at 24–48 h for Gluc activity or 2–12 h for GFP detection (rVSV-GFP and VP40-GFP) after infection. For experiments involving inhibitors or the KZ52 antibody, cells were pre-treated with appropriate concentrations of these agents for 2 h and subsequently infected with viruses in the presence of the agents throughout infection. In some cases, 293GP/LAPSN packaging cells were used to produce MLV pseudovirions bearing EBOV GP and HTX cells were used as target cells for infection; the viral titer was determined by alkaline phosphatase (AP) staining.

Isolation and purification of exosomes

Isolation of exosomes was carried out by using a referenced protocol, with minor modifications (Thery et al., 2006). Briefly, 293T donor cells were co-transfected, using a calcium phosphate method, with pQCXIP-Tet-off vector and a plasmid encoding EBOV GP. The supernatants of transfected cells were harvested 24–48 h post-transfection. Supernatants containing exosomes were clarified by centrifugation for 10 min at 300*g* and 4 °C to remove cells, followed by centrifugation for 10 min at 2000*g* and 4 °C to remove cell debris. Supernatants containing the exosomes were further clarified by ultracentrifugation for 30 min at 10,000*g* at 4 °C. Exosomes were then concentrated by ultracentrifugation for 70 min at 100,000*g* at 4 °C, and re-suspended in PBS buffer. Contaminating proteins in exosome suspensions were removed by an additional ultracentrifugation for 70 min at 100,000*g* at 4 °C. Purified exosomes were boiled in a sodium dodecyl sulfate (SDS) sample buffer for 10 min before loading to 10% SDS-PAGE electrophoresis and Western blotting. An anti-FLAG was used to detect EBOV GP and anti-CD63.

Western blotting

Cells were lysed in lysis buffer (50 mM Tris pH 7.5, 150 mM NaCl, 1 mM EDTA and 1% Triton) containing freshly added PMSF and a protease inhibitor cocktail (Sigma) for 20 min on ice. The lysates were clarified by centrifugation at 13,000*g* and 4 °C for 10 min, followed by boiling for 10 min in SDS sample buffer. Cell lysates were subjected to 7.5% or 10% SDS-PAGE electrophoresis, followed by transfer onto polyvinylidene difluoride membranes. Western blotting was performed by using specific primary antibodies, followed by appropriate secondary antibodies conjugated to horseradish peroxidase. The signals were detected by the chemiluminescence image analyzer LAS3000 (GE Healthcare Bio-Sciences, Pittsburgh, PA).

Flow cytometry

Cells were detached from dishes by adding PBS plus 5 mM EDTA, and re-suspended in PBS containing 2% FBS. Cells were then incubated with mouse anti-FLAG antibody on ice for 1 h, washed 3 times with cold PBS containing 2% FBS, and incubated with FITC conjugated anti-mouse IgG antibody for an additional 45 min. Cells were fixed and analyzed by flow cytometry.

Immunofluorescence staining and 3D de-convolution microscopy

293FT/Gluc cells stably expressing NPC1, NPC1 CT or TIM-1 were fixed with 4% paraformaldehyde, and permeabilized with 0.25% Triton X-100 for 10 min. Cells were blocked with 5% BSA, and stained with anti-FLAG antibody for 1 h. After 3 washes with PBS, cells were incubated with anti-mouse FITC for 1 h. Cells were stained with DAPI and Z-stack images were collected using a Leica DMI6000 B inverted deconvolution microscope with a 60 × oil immersion lens.

Statistical analysis

One-way ANOVA analysis of variance, with Dunnett multiple comparison methods, was used to perform all statistical tests. Unless otherwise specified, results from 3 to 6 independent experiments were used for the analysis.

Acknowledgments

We thank Marc Johnson, Kartik Chandran, James Cunningham, Dennis Burton, Erica Saphire, Paul Bates, Yoshihiro Kawaoka, Lijun Rong, David Sanders, Gary Kobinger and Gary Nabel for providing valuable reagents that make this work possible. We also thank Marceline Côté and Kartik Chandran for helpful discussions. This

work was supported by NIH grants to SLL (R21AI109464 and U54 AI057160), and to FSC (R01 GM101539).

References

Agosto, L.M., Zhong, P., Munro, J., Mothes, W., 2014. Highly active antiretroviral therapies are effective against HIV-1 cell-to-cell transmission. PLoS Pathog. 10, e1003982.

Alvarez, C.P., Lasala, F., Carrillo, J., Muniz, O., Corbi, A.L., Delgado, R., 2002. C-type lectins DC-SIGN and L-SIGN mediate cellular entry by Ebola virus in cis and in trans. J. Virol. 76, 6841–6844.

Bale, S., Liu, T., Li, S., Wang, Y., Abelson, D., Fusco, M., Woods Jr., V.L., Saphire, E.O., 2011. Ebola virus glycoprotein needs an additional trigger, beyond proteolytic priming for membrane fusion. PLoS Negl. Trop. Dis. 5, e1395.

Brecher, M., Schornberg, K.L., Delos, S.E., Fusco, M.L., Saphire, E.O., White, J.M., 2012. Cathepsin cleavage potentiates the Ebola virus glycoprotein to undergo a subsequent fusion-relevant conformational change. J. Virol. 86, 364–372.

Brimacombe, C.L., Grove, J., Meredith, L.W., Hu, K., Syder, A.J., Flores, M.V., Timpe, J.M., Krieger, S.E., Baumert, T.F., Tellinghuisen, T.L., Wong-Staal, F., Balfe, P., McKeating, J. A., 2011. Neutralizing antibody-resistant hepatitis C virus cell-to-cell transmission. J. Virol. 85, 596–605.

Brindley, M.A., Hughes, L., Ruiz, A., McCray Jr., P.B., Sanchez, A., Sanders, D.A., Maury, W., 2007. Ebola virus glycoprotein 1: identification of residues important for binding and postbinding events. J. Virol. 81, 7702–7709.

Carette, J.E., Raaben, M., Wong, A.C., Herbert, A.S., Obernosterer, G., Mulherkar, N., Kuehne, A.I., Kranzusch, P.J., Griffin, A.M., Ruthel, G., Dal Cin, P., Dye, J.M., Whelan, S.P., Chandran, K., Brummelkamp, T.R., 2011. Ebola virus entry requires the cholesterol transporter Niemann-Pick C1. Nature 477, 340–343.

Catanese, M.T., Loureiro, J., Jones, C.T., Dorner, M., von Hahn, T., Rice, C.M., 2013. Different requirements for scavenger receptor class B type I in hepatitis C virus cell-free versus cell-to-cell transmission. J. Virol. 87, 8282–8293.

Chandran, K., Sullivan, N.J., Felbor, U., Whelan, S.P., Cunningham, J.M., 2005. Endosomal proteolysis of the ebola virus glycoprotein is necessary for infection. Science 308, 1643–1645.

Côté, M., Misasi, J., Ren, T., Bruchez, A., Lee, K., Filone, C.M., Hensley, L., Li, Q., Ory, D., Chandran, K., Cunningham, J., 2011. Small molecule inhibitors reveal Niemann-Pick C1 is essential for Ebola virus infection. Nature 477, 344–348.

Côté, M., Zheng, Y.M., Albritton, L.M., Liu, S.-L., 2008. Fusogenicity of Jaagsiekte sheep retrovirus envelope protein is dependent on low pH and is enhanced by cytoplasmic tail truncations. J. Virol. 82, 2543–2554.

Dale, B.M., Alvarez, R.A., Chen, B.K., 2013. Mechanisms of enhanced HIV spread through T-cell virological synapses. Immunol. Rev. 251, 113–124.

Dowling, W., Thompson, E., Badger, C., Mellquist, J.L., Garrison, A.R., Smith, J.M., Paragas, J., Hogan, R.J., Schmaljohn, C., 2007. Influences of glycosylation on antigenicity, immunogenicity, and protective efficacy of ebola virus GP DNA vaccines. J. Virol. 81, 1821–1837.

Dube, D., Brecher, M.B., Delos, S.E., Rose, S.C., Park, E.W., Schornberg, K.L., Kuhn, J.H., White, J.M., 2009. The primed ebolavirus glycoprotein (19-kilodalton GP1,2): sequence and residues critical for host cell binding. J. Virol. 83, 2883–2891.

Feldmann, H., Geisbert, T.W., 2011. Ebola haemorrhagic fever. Lancet 377, 849–862.

Gregory, S.M., Harada, E., Liang, B., Delos, S.E., White, J.M., Tamm, L.K., 2011. Structure and function of the complete internal fusion loop from Ebolavirus glycoprotein 2. Proc. Natl. Acad. Sci. USA 108, 11211–11216.

Hoenen, T., Feldmann, H., 2014a. Ebolavirus in West Africa, and the use of experimental therapies or vaccines. BMC Biol. 12, 80.

Hoenen, T., Feldmann, H., 2014b. Reverse genetics systems as tools for the development of novel therapies against filoviruses. Expert Rev. Anti-Infect. Ther. 12, 1253–1263.

Hood, C.L., Abraham, J., Boyington, J.C., Leung, K., Kwong, P.D., Nabel, G.J., 2010. Biochemical and structural characterization of cathepsin L-processed Ebola virus glycoprotein: implications for viral entry and immunogenicity. J. Virol. 84, 2972–2982.

Hunt, C.L., Kolokoltsov, A.A., Davey, R.A., Maury, W., 2011. The Tyro3 receptor kinase Axl enhances macropinocytosis of Zaire ebolavirus. J. Virol. 85, 334–347.

Janaka, S.K., Gregory, D.A., Johnson, M.C., 2013. Retrovirus glycoprotein functionality requires proper alignment of the ectodomain and the membrane-proximal cytoplasmic tail. J. Virol. 87, 12805–12813.

Jeffers, S.A., Sanders, D.A., Sanchez, A., 2002. Covalent modifications of the ebola virus glycoprotein. J. Virol. 76, 12463–12472.

Jin, J., Sherer, N.M., Heidecker, G., Derse, D., Mothes, W., 2009. Assembly of the murine leukemia virus is directed towards sites of cell-cell contact. PLoS Biol. 7, e1000163.

Kaletsky, R.L., Simmons, G., Bates, P., 2007. Proteolysis of the Ebola virus glycoproteins enhances virus binding and infectivity. J. Virol. 81, 13378–13384.

Kondratowicz, A.S., Lennemann, N.J., Sinn, P.L., Davey, R.A., Hunt, C.L., Moller-Tank, S., Meyerholz, D.K., Rennert, P., Mullins, R.F., Brindley, M., Sandersfeld, L.M., Quinn, K., Weller, M., McCray Jr., P.B., Chiorini, J., Maury, W., 2011. T-cell immunoglobulin and mucin domain 1 (TIM-1) is a receptor for Zaire Ebolavirus and Lake Victoria Marburgvirus. Proc. Natl. Acad. Sci. USA 108, 8426–8431.

Lee, J.E., Fusco, M.L., Hessell, A.J., Oswald, W.B., Burton, D.R., Saphire, E.O., 2008. Structure of the Ebola virus glycoprotein bound to an antibody from a human survivor. Nature 454, 177–182.

Li, M., Ablan, S.D., Miao, C., Zheng, Y.M., Fuller, M.S., Rennert, P.D., Maury, W., Johnson, M.C., Freed, E.O., Liu, S.L., 2014. TIM-family proteins inhibit HIV-1 release. Proc. Natl. Acad. Sci. USA 111, E3699–E3707.

Lin, G., Simmons, G., Pohlmann, S., Baribaud, F., Ni, H., Leslie, G.J., Haggarty, B.S., Bates, P., Weissman, D., Hoxie, J.A., Doms, R.W., 2003. Differential N-linked glycosylation of human immunodeficiency virus and Ebola virus envelope glycoproteins modulates interactions with DC-SIGN and DC-SIGNR. J. Virol. 77, 1337–1346.

Madison, M.N., Okeoma, C.M., 2015. Exosomes: implications in HIV-1 Pathogenesis. Viruses 7, 4093–4118.

Mangeot, P.E., Dollet, S., Girard, M., Ciancia, C., Joly, S., Peschanski, M., Lotteau, V., 2011. Protein transfer into human cells by VSV-G-induced nanovesicles. Mol. Ther.: J. Am. Soc. Gene Ther. 19, 1656–1666.

Manicassamy, B., Wang, J., Jiang, H., Rong, L., 2005. Comprehensive analysis of ebola virus GP1 in viral entry. J. Virol. 79, 4793–4805.

Marzi, A., Akhavan, A., Simmons, G., Gramberg, T., Hofmann, H., Bates, P., Lingappa, V.R., Pohlmann, S., 2006. The signal peptide of the ebolavirus glycoprotein influences interaction with the cellular lectins DC-SIGN and DC-SIGNR. J. Virol. 80, 6305–6317.

Miller, E.H., Obernosterer, G., Raaben, M., Herbert, A.S., Deffieu, M.S., Krishnan, A., Ndungo, E., Sandesara, R.G., Carette, J.E., Kuehne, A.I., Ruthel, G., Pfeffer, S.R., Dye, J.M., Whelan, S.P., Brummelkamp, T.R., Chandran, K., 2012. Ebola virus entry requires the host-programmed recognition of an intracellular receptor. EMBO J. 31, 1947–1960.

Misasi, J., Chandran, K., Yang, J.Y., Considine, B., Filone, C.M., Cote, M., Sullivan, N., Fabozzi, G., Hensley, L., Cunningham, J., 2012. Filoviruses require endosomal cysteine proteases for entry but exhibit distinct protease preferences. J. Virol. 86, 3284–3292.

Nanbo, A., Imai, M., Watanabe, S., Noda, T., Takahashi, K., Neumann, G., Halfmann, P., Kawaoka, Y., 2010. Ebolavirus is internalized into host cells via macropinocytosis in a viral glycoprotein-dependent manner. Plos Pathog. 6, e1001121.

Ou, W., King, H., Delisle, J., Shi, D., Wilson, C.A., 2010. Phenylalanines at positions 88 and 159 of Ebolavirus envelope glycoprotein differentially impact envelope function. Virology 396, 135–142.

Parren, P.W., Geisbert, T.W., Maruyama, T., Jahrling, P.B., Burton, D.R., 2002. Pre- and post-exposure prophylaxis of Ebola virus infection in an animal model by passive transfer of a neutralizing human antibody. J. Virol. 76, 6408–6412.

Qiu, X., Wong, G., Audet, J., Bello, A., Fernando, L., Alimonti, J.B., Fausther-Bovendo, H., Wei, H., Aviles, J., Hiatt, E., Johnson, A., Morton, J., Swope, K., Bohorov, O., Bohorova, N., Goodman, C., Kim, D., Pauly, M.H., Velasco, J., Pettitt, J., Olinger, G.G., Whaley, K., Xu, B., Strong, J.E., Zeitlin, L., Kobinger, G.P., 2014. Reversion of advanced Ebola virus disease in nonhuman primates with ZMapp. Nature 514, 47–53.

Ramakrishnaiah, V., Thumann, C., Fofana, I., Habersetzer, F., Pan, Q., de Ruiter, P.E., Willemsen, R., Demmers, J.A., Stalin Raj, V., Jenster, G., Kwekkeboom, J., Tilanus, H. W., Haagmans, B.L., Baumert, T.F., van der Laan, L.J., 2013. Exosome-mediated transmission of hepatitis C virus between human hepatoma Huh7.5 cells. Proc. Natl. Acad. Sci. USA 110, 13109–13113.

Roberts, K.L., Manicassamy, B., Lamb, R.A., 2015. Influenza A virus uses intercellular connections to spread to neighboring cells. J. Virol. 89, 1537–1549.

Saeed, M.F., Kolokoltsov, A.A., Albrecht, T., Davey, R.A., 2010. Cellular entry of ebola virus involves uptake by a macropinocytosis-like mechanism and subsequent trafficking through early and late endosomes. PLoS Pathog. 6, e1001110.

Schornberg, K., Matsuyama, S., Kabsch, K., Delos, S., Bouton, A., White, J., 2006. Role of endosomal cathepsins in entry mediated by the ebola virus glycoprotein. J. Virol. 80, 4174–4178.

Simmons, G., Wool-Lewis, R.J., Baribaud, F., Netter, R.C., Bates, P., 2002. Ebola virus glycoproteins induce global surface protein down-modulation and loss of cell adherence. J. Virol. 76, 2518–2528.

Takada, A., Robison, C., Goto, H., Sanchez, A., Murti, K.G., Whitt, M.A., Kawaoka, Y., 1997. A system for functional analysis of Ebola virus glycoprotein. Proc. Natl. Acad. Sci. USA 94, 14764–14769.

Thery, C., Amigorena, S., Raposo, G., Clayton, A., 2006. Isolation and characterization of exosomes from cell culture supernatants and biological fluids (Chapter 3). In: Bonifacino, Juan S. (Ed.), Current Protocols in Cell Biology/Editorial Board, p. 22.

Trajkovic, K., Hsu, C., Chiantia, S., Rajendran, L., Wenzel, D., Wieland, F., Schwille, P., Brugger, B., Simons, M., 2008. Ceramide triggers budding of exosome vesicles into multivesicular endosomes. Science 319, 1244–1247.

Tscherne, D.M., Garcia-Sastre, A., 2011. An enzymatic assay for detection of viral entry (Chapter 26). In: Bonifacino, Juan S. (Ed.), Current Protocols in Cell Biology/Editorial Board, p. 12.

Wang, J., Manicassamy, B., Caffrey, M., Rong, L., 2011. Characterization of the receptor-binding domain of Ebola glycoprotein in viral entry. Virol. Sin. 26, 156–170.

Warren, T.K., Wells, J., Panchal, R.G., Stuthman, K.S., Garza, N.L., Van Tongeren, S.A., Dong, L., Retterer, C.J., Eaton, B.P., Pegoraro, G., Honnold, S., Bantia, S., Kotian, P., Chen, X., Taubenheim, B.R., Welch, L.S., Minning, D.M., Babu, Y.S., Sheridan, W.P., Bavari, S., 2014. Protection against filovirus diseases by a novel broad-spectrum nucleoside analogue BCX4430. Nature 508, 402–405.

Watanabe, S., Takada, A., Watanabe, T., Ito, H., Kida, H., Kawaoka, Y., 2000. Functional importance of the coiled-coil of the Ebola virus glycoprotein. J. Virol. 74, 10194–10201.

White, J.M., Delos, S.E., Brecher, M., Schornberg, K., 2008. Structures and mechanisms of viral membrane fusion proteins: multiple variations on a common theme. Crit. Rev. Biochem. Mol. Bio 43, 189–219.

White, J.M., Schornberg, K.L., 2012. A new player in the puzzle of filovirus entry. Nat. Rev. Microbiol. 10, 317–322.

Wong, A.C., Sandesara, R.G., Mulherkar, N., Whelan, S.P., Chandran, K., 2010. A forward genetic strategy reveals destabilizing mutations in the Ebolavirus glycoprotein that alter its protease dependence during cell entry. J. Virol. 84, 163–175.

Wool-Lewis, R.J., Bates, P., 1999. Endoproteolytic processing of the ebola virus envelope glycoprotein: cleavage is not required for function. J. Virol. 73, 1419–1426.

Yonezawa, A., Cavrois, M., Greene, W.C., 2005. Studies of ebola virus glycoprotein-mediated entry and fusion by using pseudotyped human immunodeficiency virus type 1 virions: involvement of cytoskeletal proteins and enhancement by tumor necrosis factor alpha. J. Virol. 79, 918–926.

Zhong, P., Agosto, L.M., Munro, J.B., Mothes, W., 2013. Cell-to-cell transmission of viruses. Curr. Opin. Virol. 3, 44–50.